$AgIn_2/Ag_2In$ Transformations in an In-49Sn/Ag Soldered Joint under Thermal Aging

T.H. CHUANG, Y.T. HUANG, and L.C. TSAO

National Taiwan University, Institute of Materials Science and Engineering, Taipei 106, Taiwan

The interfacial reaction between liquid In-49Sn solders and Ag substrates results in the formation of a thicker Ag_2In intermetallic compound accompanied with the development of a thin $AgIn_2$ layer. Through further aging of the In-49Sn/Ag soldered specimens at various temperatures ranging from room to 100°C, solid/solid transitions between Ag_2In and $AgIn_2$ intermetallic compounds can be observed. When the temperature drops below 75°C, Ag_2In will react with the In-49Sn solder to form the dominant $AgIn_2$ phase. Conversely, $AgIn_2$ is consumed at a higher temperature (e.g., 100°C) when reacting with the Ag substrate to create a now dominant Ag_2In phase. Lastly, the different mechanical, electrical, magnetic, and corrosion behaviors of both intermetallic compounds are respectively made known through direct measurements of the material properties of the individual Ag_2In and $AgIn_2$ bulk samples.

Key words: In-49Sn solders, Ag substrate, aging, solid/solid transformations

INTRODUCTION

In-Sn solders possess the advantages of greater ductility and longer fatigue life than the more traditional Pb-Sn solders.[1–5] Gold embrittlement failures in advanced packaging can specifically be prevented by taking advantage of the lower solubility of Au in In-Sn solders.[6] Also, the alloy's lower melting point can be favorable in electronic packaging hierarchy. The interfacial reaction, between liquid In-Sn solders and Cu substrates has been intensively studied,[7,8] showing a multilayer structure of the reaction product: $Cu/Cu_2(Sn,In)/Cu_2In_3Sn/InSn$. Shohji et al.[9] reported that a $AuIn_2$ layer and a γ-phase layer formed during the interfacial reaction between Au and the In-48Sn solder. The activation energy for the formation of $AuIn_2$ was 42.8 KJ/mol, equivalent to the activation energy for the diffusion of Au atoms in $AuIn_2$. Lin et al.[10] studied a variety of solders (20In-80Sn, 51In-49Sn, and 80In-20Sn) reacting with an electroless plated Ni-P layer to form Ni_2In_3, followed by the ensuing dissolution of Sn in the intermetallic compound after aging at 60°C.

In previous work by two of the authors of this present study, the interfacial reaction between liquid In-49Sn solders and Ag substrates was investigated.[11] The reaction product at the In-49Sn(I)/Ag(s) interface was Ag_2In enveloped in a thin shell of $AgIn_2$. During such a liquid/solid reaction, the thickness of the $AgIn_2$ intermetallic compound remained constant. Further study showed that the microstructure of the interfacial intermetallic compounds had undergone more transformation when the In-49Sn solder remained solid and aged for a number of days at room temperature. During the solid/solid reaction at room temperature, the $AgIn_2$ grew by consumption of the Ag_2In phase. In contrast, at about 100°C, the $AgIn_2$ intermetallic compound diminished with the growth of Ag_2In. Such a phenomenon is important to application, for an elevation of temperature in the solder joints is inevitable in the operations of any electronic device. The efforts of this study are focused on the morphology and kinetics of the solid/solid reactions at the In-49Sn/Ag soldered interface from room temperature to 100°C. To evaluate the influence of such reactions on solder joint reliability, mechanical, electrical, magnetic, and corrosion properties of the individual $AgIn_2$ and Ag_2In intermetallic alloys are also investigated.

(Received November 6, 2000; accepted April 5, 2001)

EXPERIMENTAL

Silver substrates (8 mm × 12 mm) were cut from a 1 mm-thick high-purity silver plate (Ag-99.95%), ground with 1500 grit SiC paper, and polished with 1 μm and 0.3 μm Al_2O_3 powders. The In-49Sn solder was prepared by vacuum melting into an ingot and ho-

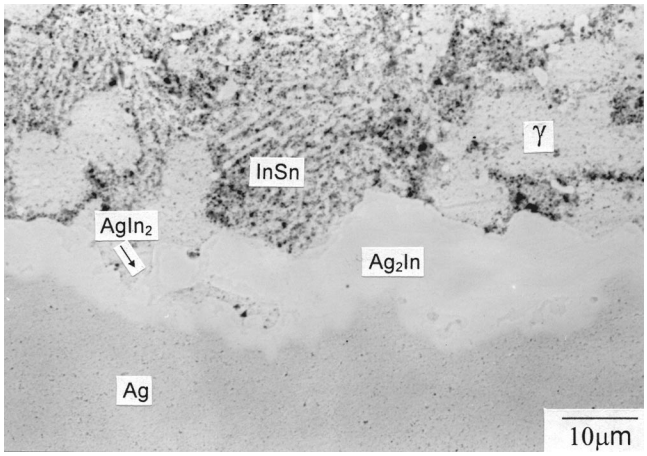

Fig. 1. Morphology of the original reaction products at the In-49Sn/Ag soldered interface (soldering reaction: 225°C, 50 min).

mogenized at 100°C for 50 hr and was rolled into a 0.2 mm-thick foil. For observing the solid/liquid interfacial reactions, the solder foil was cut to the same size as the silver substrate, placed on the silver substrate, and then heated at 225°C for 50 min in an infrared furnace under a vacuum of 10^{-3} torr. To eliminate oxidation of the solder, a flux was applied before testing. Further aging treatments were performed at room temperature, 50°C, 75°C, and 100°C for various periods of time.

To observe the morphology of the intermetallic compounds after reaction, specimens were cut in cross-sections, ground with SiC paper, polished with 1 μm and 0.3 μm Al_2O_3 powders, and examined in the scanning electron microscope (SEM). The width of the intermetallic layer was also directly measured on the screen because the intermetallic compounds grew unevenly and did not remain planar. The thickness of an intermetallic layer was determined by measuring the layer thickness at 50 equally-spaced points and calculating the average thickness. The standard deviation for various intermetallic compound layers was between 0.5 μm and 1.5 μm. The composition of the intermetallic compounds formed during the reactions was analyzed by an electron-probe microanalyzer (EPMA).

Since it is very difficult to measure the physical properties of the individual intermetallic layers at the reacted interface, a rough estimate was conducted with the bulk samples of the related intermetallic phases. For this purpose, both monolithic intermetallic alloys with the stoichiometric compositions of Ag_2In and $AgIn_2$ were cast in a vacuum furnace, and homogenized at 120°C for 1000 hr. After homogenization, both intermetallic bulk materials showed a single-phase and equiaxial polycrystalline microstructure. The grain sizes of the Ag_2In and $AgIn_2$ alloys were 45 μm and 68 μm, respectively. The metallographic observations of the solder In-49Sn/Ag soldered samples showed that the interfacial reaction products were of a scallop-shaped Ag_2In phase enveloped in an outer layer of the $AgIn_2$ phase. Both were identified as single crystals using polarized light under an optical microscope. The width of the Ag_2In scallops wrapped in an outer $AgIn_2$ layer ranged from 20 μm to 60 μm, which was near the grain size of the bulk samples. The microstructures of the respective intermetallics at the In-49Sn/Ag interface in the interfacial prod-

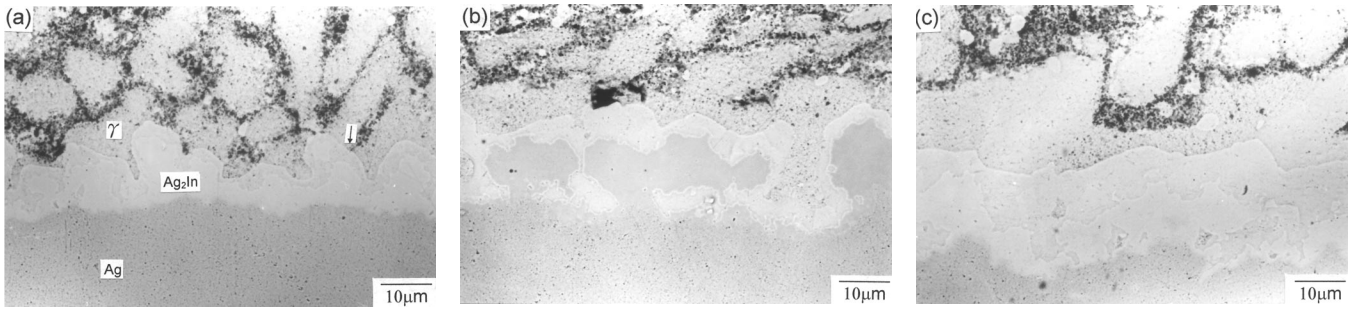

Fig. 2. Morphology of the reaction products at the In-49Sn/Ag soldered interface after aging at room temperature for various time periods: (a) 10 days, (b) 23 days, (c) 60 days.

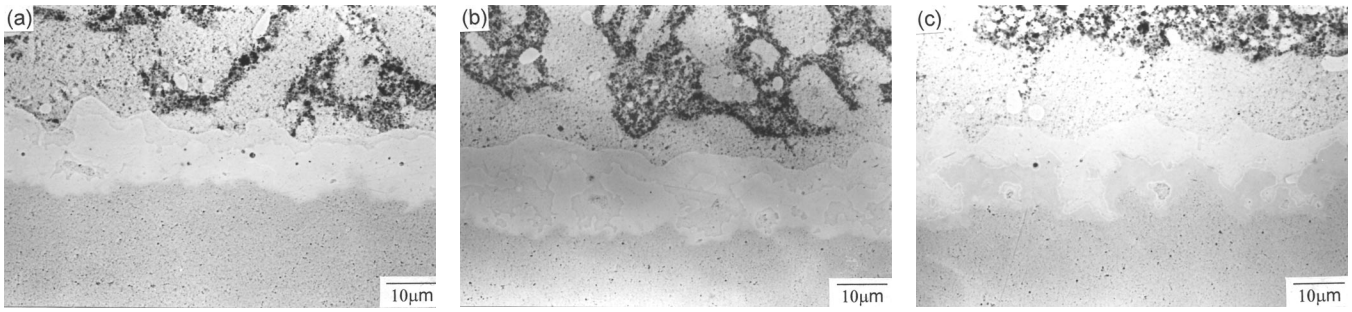

Fig. 3. Morphology of the reaction products at the In-49Sn/Ag soldered interface after aging at 50°C for various time periods: (a) 5 days, (b) 10 days, (c) 23 days.

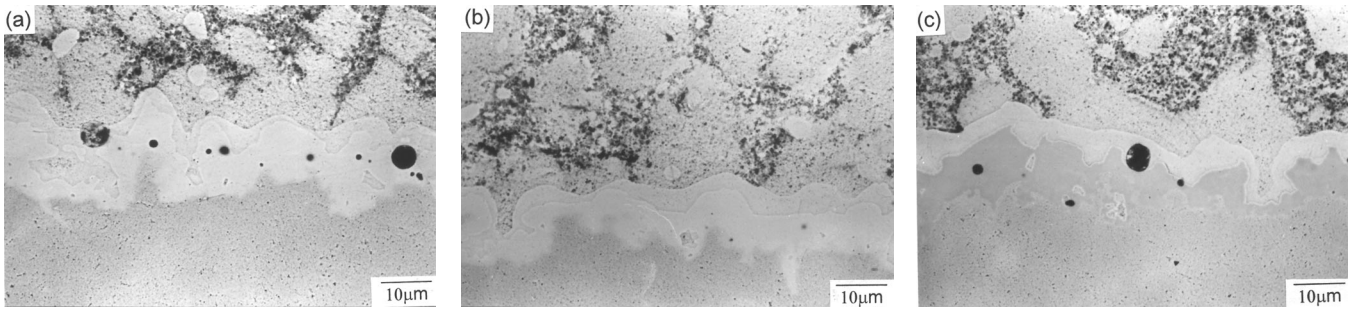

Fig. 4. Morphology of the reaction products at the In-49Sn/Ag soldered interface after aging at 75°C for various time periods: (a) 5 days, (b) 10 days, (c) 23 days.

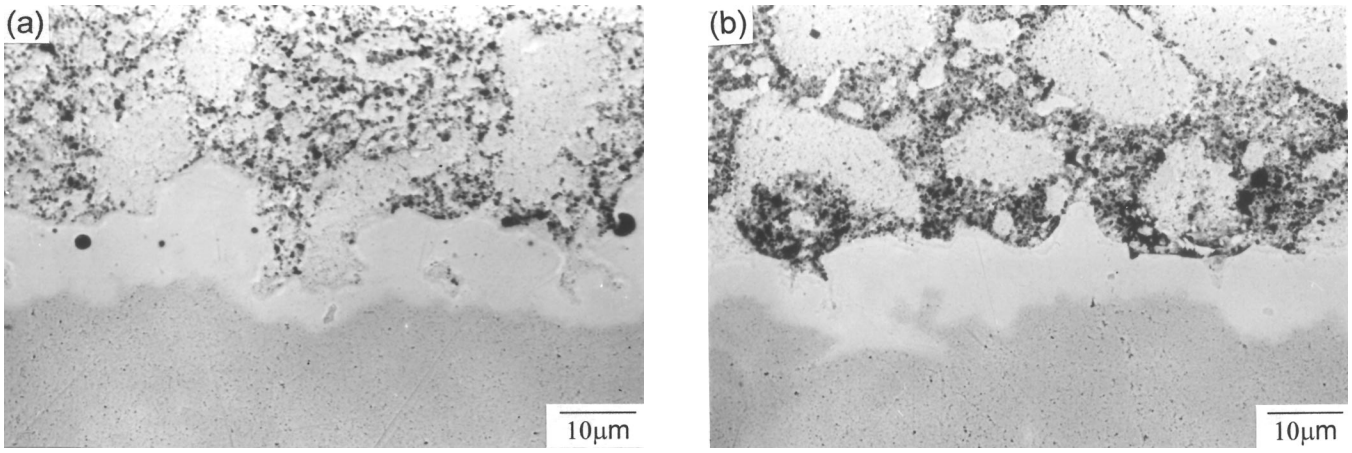

Fig. 5. Morphology of the reaction products at the In-49Sn/Ag soldered interface after aging at 100°C for various time periods: (a) 5 days, (b) 10 days.

ucts and in the bulk samples were quite similar, which implied that the measurements of mechanical, electrical, magnetic, and corrosion properties using the bulk intermetallic samples could somewhat represent the corresponding properties of intermetallic phases in the In-49Sn/Ag-soldered specimens. The electrical resistivity of both intermetallic compounds was determined by applying the conventional four-probe technique in the temperature range between –263°C and 27°C. Magnetization was measured in the same temperature range by a vibrating sample magnetometer.

The corrosion properties of both intermetallic compounds were examined at room temperature in a

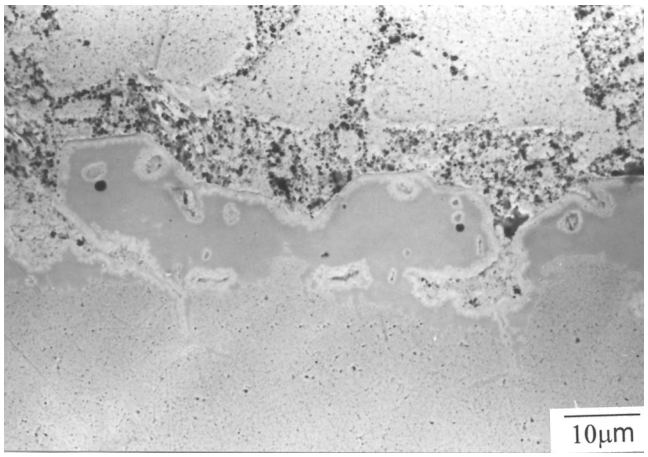

Fig. 6. Morphology of the reaction products at the In-49Sn/Ag soldered interface after aging at room temperature for 72 days and further at 100°C for 1 day.

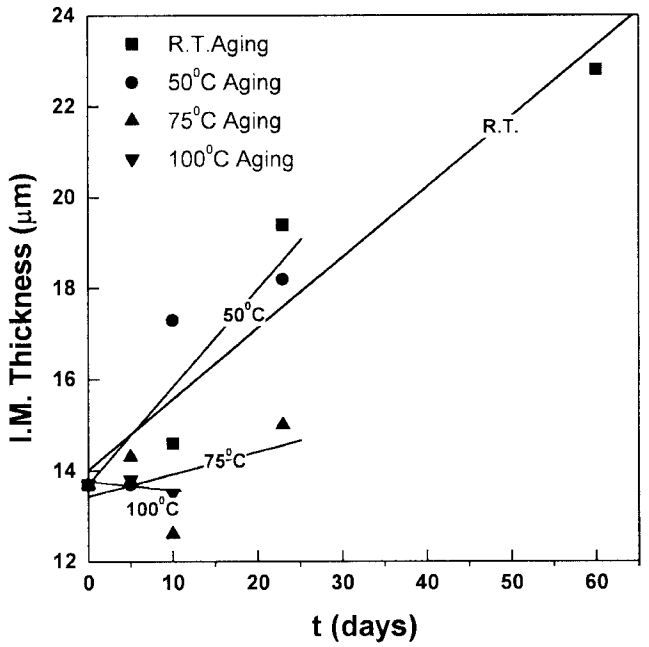

Fig. 7. Sum total of I.M. thickness (Ag_2In thickness + $AgIn_2$ thickness) in relevance to the time factor for the aging of the In-49Sn/Ag solder joint in Fig. 1.

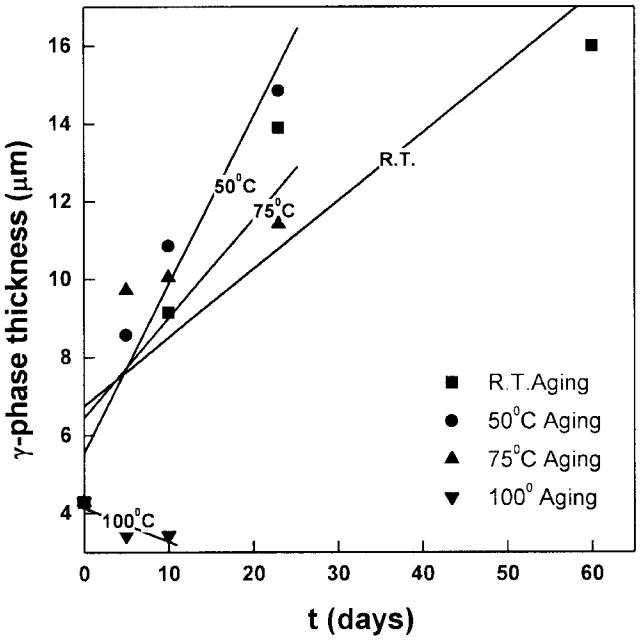

Fig. 8. Thickness of the γ-phase ahead of Ag_2In in relevance to the time factor for the aging of the In-49Sn/Ag solder joint in Fig. 1.

3.5 wt.% NaCl solution using a potentiostat. Prior to testing, the specimens were ground with 1200# grit SiC paper and cleaned in acetone for 2 min. For dynamic polarization testing, the potential began at –1800 mV vs. saturated calomel electrode and was scanned in the noble direction to an anodic current density of 10^4 μA/cm² at a scanning rate of 1 mV/s.

RESULTS AND DISCUSSION

Figure 1 shows the morphology of intermetallic compounds formed at the In-49Sn/Ag interface after soldering reaction at 225°C for 50 min. The Ag_2In phase appears at the interface with a thickness of about 12 μm. Between Ag_2In and the In-49Sn solder, a continuous thin layer of $AgIn_2$ with a thickness of about 1 μm is observed. Clusters of the Sn-rich γ-phase exist in areas ahead of the Ag_2In and $AgIn_2$ intermetallic compounds. The kinetics of such a soldering reaction has been analyzed previously.[11]

When such post-soldering-reaction specimens age at room temperature for 10, 23, and 60 days, a change in the morphology of intermetallic compounds at the In-49Sn/Ag interface takes place, as shown in Fig. 2. Along with the increase of aging time at this temperature, the aggregate thickness of both intermetallic compounds (Ag_2In + $AgIn_2$) increases due to further solid/solid reactions between the In-49Sn solder and the Ag substrate. Also, the γ-phase emerges and grows in front of the intermetallic compounds as a result of the excess Sn atoms repelled from the interfacial reaction layer into the In-49Sn solder. As the thicknesses of the Ag_2In and $AgIn_2$ phases are placed in comparison, it is evident that the formerly created thin $AgIn_2$ layer grows, and consumes the Ag_2In phase. This phenomenon also occurs in the In-49Sn/Ag specimens with aging treatments at 50°C and 75°C, as shown in Figs. 3 and 4. However, when the aging temperature increases to 100°C, this transformation is reversed for both intermetallic compounds. The thin $AgIn_2$ layer diminishes as the Ag_2In phase expands (see Fig. 5). The In-49Sn/Ag specimens were aged at room temperature for 72 days to achieve a sufficient thickness of the $AgIn_2$ phase, and then further aged at 100°C for one more day. Figure 6 shows that the thick $AgIn_2$ layer formed at room temperature is transformed back into the Ag_2In phase.

Quantitative measurements of the thicknesses of individual phases (Ag_2In, $AgIn_2$ and the γ-phase) at the In-49Sn/Ag soldered interface after aging at various temperatures are shown in Table I. The results are plotted as a function of aging time to clarify the

Table I. Quantitative Measurements of the Thickness of Ag_2In and $AgIn_2$ and the γ-phase in the In-49Sn/Ag Solder Joint After Aging at Various Temperatures for Various Periods of Time

Aging Conditions	Ag_2In Thickness (μm)	$AgIn_2$ Thickness (μm)	I.M. Thickness* (μm)	Ag_2In Thickness I.M. Thickness	γ Thickness (μm)
225°C, 50 min	12.6	1.1	13.7	91.8%	4.3
R.T., 10 days	11.1	3.4	14.6	76.3%	9.1
R.T., 23 days	10.3	9.1	19.4	53.0%	1.9
R.T., 60 days	9.1	13.7	22.8	40.0%	16.0
50°C, 5 days	9.2	4.6	13.7	66.8%	8.6
50°C, 10 days	8.1	9.2	17.3	46.9%	10.9
50°C, 23 days	7.9	10.3	18.2	43.4%	14.9
75°C, 5 days	7.9	4.7	12.6	59.9%	9.7
75°C, 10 days	8.6	5.7	14.3	62.6%	10.0
75°C, 23 days	8.1	6.9	15.0	54.1%	11.4
100°C, 5 days	13.4	0.4	13.8	97.2%	4.0
100°C, 10 days	13.0	0.5	13.5	96.4%	3.4
R.T., 72 days and 100°C, 1 day	12.8	1.4	14.2	90.1%	3.0

* I.M. thickness = Ag_2In thickness + $AgIn_2$ thickness

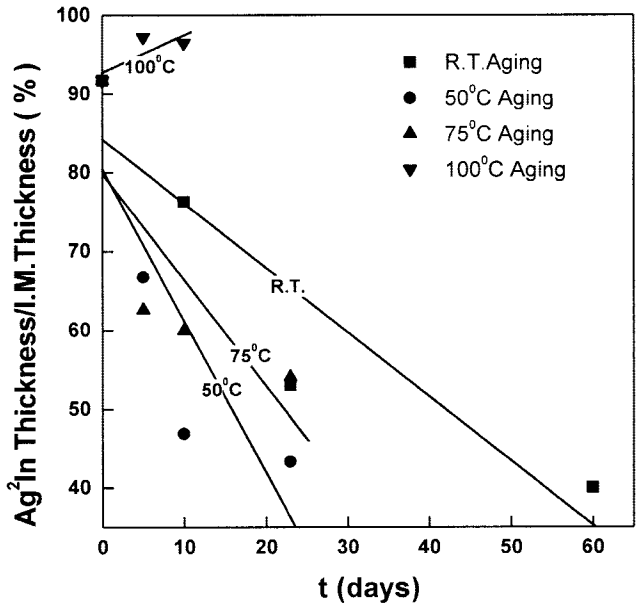

Fig. 9. Proportion of Ag_2In thickness to the total I.M. thickness in relevance to the time factor for the aging of the In-49Sn/Ag solder joint in Fig. 1.

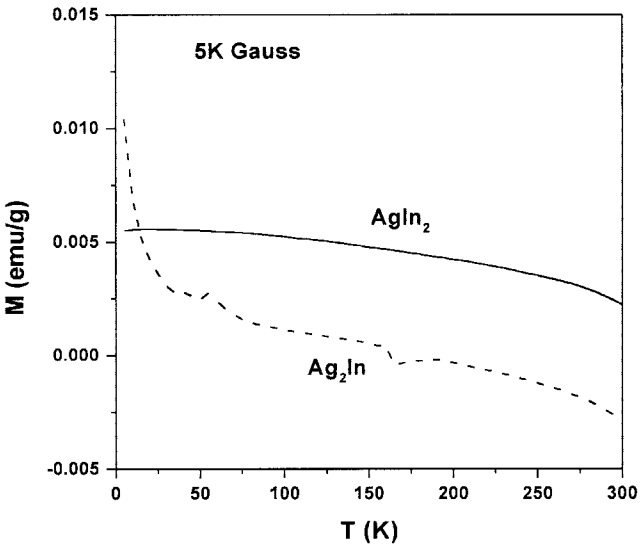

Fig. 11. Comparisons of the magnetization of Ag_2In and $AgIn_2$ intermetallic compounds at 5 K Gauss in the temperature range between –263°C and 27°C.

Table II. Corrosion Data of Ag_2In and $AgIn_2$ Intermetallic Compounds Obtained from the Polarization Curves in Figure 12

Specimens	Φ_{corr} (mV)	I_{corr} ($\mu A/cm^2$)	Φ_b (mV)	$\Delta\Phi$ (mV)
Ag_2In	–274	0.75	–61	213
$AgIn_2$	–1026	6.55	–682	344

Φ_{corr}—corrosion potential; I_{coor}—corrosion current density; Φ_b—breakdown potential; $\Delta\Phi = \Phi_b - \Phi_{corr.}$

growth tendency at various aging temperatures. Figure 7 shows that the aggregate thickness of both intermetallic compounds (Ag_2In + $AgIn_2$) increases

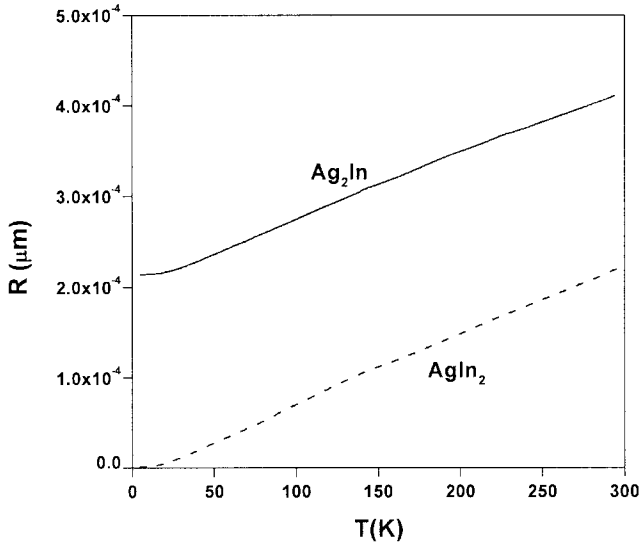

Fig. 10. Comparisons of the electrical resistance of Ag_2In and $AgIn_2$ intermetallic compounds in the temperature range between –263°C and 27°C.

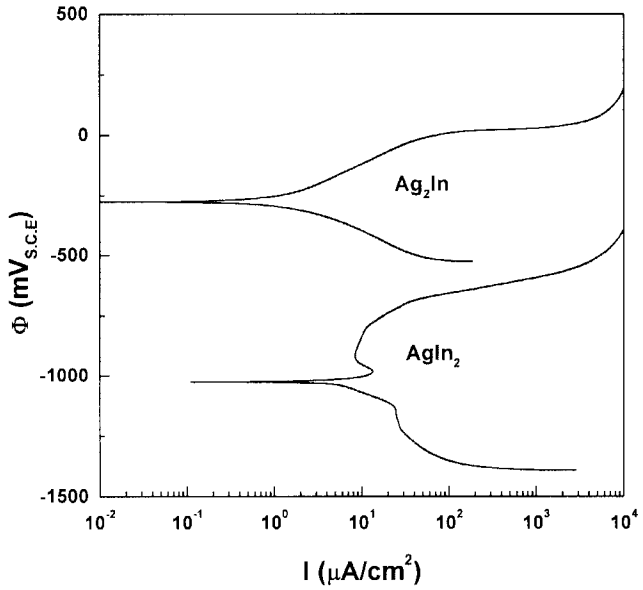

Fig. 12. Comparisons of the corrosion polarization curves of Ag_2In and $AgIn_2$ intermetallic compounds in a 3.5 wt.% NaCl solution at room temperature.

with aging time when the aging temperatures remain below 75°C. The growth rate increases as the aging temperature increases from room temperature to 50°C and then declines with any further increase in aging temperature up to 75°C. Instead of phase growth, the aggregate thickness of intermetallic compounds (Ag_2In + $AgIn_2$) remains somewhat constant during aging at 100°C. Similar tendencies of phase growth in relation to the aging temperature can be found in Fig. 8, where the γ-phase thickness is shown. The proportion of Ag_2In thickness to the total intermetallic compound (I.M.) thickness (Ag_2In thickness + $AgIn_2$ thickness) is calculated for all specimens and given in Table I. The results plotted in Fig. 9 reflect morphological observations of the transformations

of intermetallic compounds at the In-49Sn/Ag soldered interface after aging at various temperatures. The Ag_2In and $AgIn_2$ phases compete for growth at various aging temperatures. Below 75°C, the dominant phase is $AgIn_2$ and a solid/solid reaction occurs between the Ag_2In intermetallic compound and the In-49Sn solder: $Ag_2In + 3In \rightarrow 2AgIn_2$. On the other hand, the Ag_2In phase becomes dominant at higher aging temperatures (e.g., 100°C for this study). In the latter case, the $AgIn_2$ intermetallic compound reacts with the Ag substrate and transforms into the Ag_2In phase: $AgIn_2 + 3Ag \rightarrow 2Ag_2In$.

An electronic solder joint encounters various temperatures when the electronic device is in operation. The switching of dominant roles for the intermetallic compounds (Ag_2In and $AgIn_2$) at the In-49Sn/Ag soldered interface affects the material properties and the reliability of the solder joint in question. For a rough estimate of the material properties of the intermetallic phases at the In-49Sn/Ag interface, the monolithic Ag_2In and $AgIn_2$ bulk specimens were prepared, and their mechanical, electrical, magnetic, and corrosion properties evaluated. Both intermetallic compounds were found to possess different microhardness values. The Ag_2In was 122.8 Hv, harder than that of $AgIn_2$ (78.9 Hv). Figures 10 and 11 show that the Ag_2In intermetallic compound possesses a higher electrical resistance and a lower magnetization. The polarization curves obtained from both intermetallic compounds in a 3.5%NaCl solution are shown in Fig. 12. The corrosion data are given in Table II. In comparison with the results obtained for $AgIn_2$, the Ag_2In intermetallic compound displays a more noble corrosion potential, which is attributed to the higher content of the noble Ag element in this alloy. However, the results also indicate that the Ag_2In intermetallic compound possesses a higher pitting tendency (smaller $\Delta\Phi$ value) and a slightly higher corrosion current density.

CONCLUSIONS

After soldering reaction between In-49Sn and the Ag substrate at 225°C for 50 min, there appears a 12 μm-thick Ag_2In intermetallic compound enveloped in a continuous thin layer of $AgIn_2$. By further aging the In-49Sn/Ag soldered specimens at various temperatures ranging from room to 100°C, the Ag_2In and $AgIn_2$ intermetallic compounds compete for a dominant role. At lower temperatures below 75°C, the $AgIn_2$ expands in proportion to the consumption of the Ag_2In phase. The dominant reaction is: $Ag_2In + 3In \rightarrow 2AgIn_2$. At higher aging temperatures above 75°C, another type of solid/solid reaction becomes dominant: $AgIn_2 + 3Ag \rightarrow 2Ag_2In$. Monolithic Ag_2In and $AgIn_2$ bulk samples have been prepared, and their material properties evaluated. Experimental results show that Ag_2In displays much greater microhardness, higher electrical resistance, lower magnetization, and lower corrosion resistance than $AgIn_2$. Although the intermetallic phases at the In-49Sn/Ag interface appear as thin films, they possess a similar microstructure of single phase and near grain size as the respective bulk materials. The results obtained from bulk samples could somewhat reflect the fact that different interfacial intermetallic compounds dominating at different aging temperatures in this study would possess different material properties, which should be taken into consideration in the application of the In-49Sn/Ag solder joints.

REFERENCES

1. Z. Mei and J. W. Morris, *J. Electron. Mater.* 21, 599 (1992).
2. S.K. Kang and A.K. Sarkhel, *J. Electron. Mater.* 23, 701 (1994).
3. J. Glazer, *Int. Mater. Rev.* 40, 65 (1995).
4. Z. Mei and J.W. Morris, *J. Electron. Mater.* 21, 401 (1992).
5. K. Shimizu, T Nakanishi, K. Karasawa, K. Hashimoto, and K. Niwa, *J. Electron. Mater.* 25, 39 (1996).
6. N.C. Lee, *Sold. Surf. Mount Technol.* 26, 65 (1997).
7. J.W. Morris, Jr., J.L.F. Goldstein, and Z. Mei, *J. Electron. Mater.* 22, 25 (1993).
8. A.D. Romig, F.G. Yost, and P.F. Hlava, *Proc. Conf. Microbeam Analysis* (San Francisco, CA: San Francisco Press, 1984), p. 87.
9. I. Shohji, S. Fujiwara, S. Kiyono, and K.F. Kobayashi, *Scri. Mater.* 40, 815 (1999).
10. K.L. Lin and C.J. Chen, *J. Mater. Sci.: Mater. in Electron.* 7, 397 (1996).
11. Y.T. Huang and T.H. Chuang, *Z. Metallkd.* 12, 1002 (2000).